

Cyclic Fatigue Resistance of Three Different Rotary Endodontic Instruments with Design Modification

Ali S Abu Naila^{*}, Hussain F Al-Huwaizi

Department of Conservative and Esthetic Dentistry, University of Dentistry-Baghdad, Iraq

ABSTRACT

Background: CF (Cyclic Fatigue) resistance of Dentsply Pro Taper Universal (PTU), Pro Taper Gold (PTG), and Pro Taper Next (PTN) nickel titanium (NiTi) rotary files was evaluated in comparison with simulated files with same design and our study design.

Methods: For PTU and PTG study design modification is to leave the apical 8 mm of S1 and the apical 3 mm of S2 as un-milled, F1 only the apical 5 mm would have cutting blades. For PTN is to leave the apical 8 mm of X1 and, while for X2 is to leave the coronal 8 mm as un-milled. Ten instruments for each file (S1, S2, F1, X1 and X2); total 240 files (80 pieces for Dentsply, 80 pcs for simulated and 80 pieces for study design), files rotated in simulated canal until fracture.

Conclusion: PTG instruments were most resistant to CF, followed by PTN and PTU. S1 and S2 files making the non-active part plane will increase CF resistance while for F1 files will decrease CF resistance. For PTN files groups, for X1 files making the non-active part plane will increase CF resistance while for X2 files will decrease CF resistance.

Key words: Cyclic, Fatigue, Gold, Next, Pro taper, Universal, Simulated, Study

HOW TO CITE THIS ARTICLE: Ali S Abu Naila, Hussain F Al-Huwaizi, Cyclic Fatigue Resistance of Three Different Rotary Endodontic Instruments with Design Modification, J Res Med Dent Sci, 2022, 10 (8): 001-010.

Corresponding author: Ali S Abu Naila

E-mail: ali.mario28@yahoo.com

Received: 20-May-2022, Manuscript No. JRMDs-22-43723;

Editor assigned: 23-May-2022, Pre QC No. JRMDs-22-43723 (PQ);

Reviewed: 06-Jun-2022, QC No. JRMDs-22-43723;

Revised: 25-Jul-2022, Manuscript No. JRMDs-22-43723 (R);

Published: 01-Aug-2022

INTRODUCTION

Due to the errors in techniques caused by stainless steel files, the innovation of Nickel-Titanium (NiTi) for production of rotary endodontic files [1]. The necessary characteristics of NiTi rotary files are shape memory, great flexibility, and preserving the original shape of the canal during preparation of the canal. Peculiarly, elasticity of NiTi files is double or triple higher times than stainless-steel files because the modulus of elasticity of nickel titanium is low [2,3]. The substance characteristics of NiTi and stainless-steel rotary instruments are presented in

Table 1. Despite the great elasticity of NiTi rotary files, fracture also happened [4,5]. The cause of rotary NiTi files failure is either by flexural fracture (cyclic fatigue) or torsional fracture [6]. Research workers revealed that flexural fracture occurs during the flexion of the endodontic file at the highest area of curvature in the canal at time of rotation when the file is compressed and tensioned multiple times [5,7]. At the curvature outer wall, the file is tensioned while at the curvature inner wall, the file is compressed. Flexural fracture of the file happened during the rotation in multiple cycles at the curvature part of the canal. While torsional fracture occurred when whole part of the file keeps rotating while tip of the file locked inside the canal. So, the tip will be fractured when the elastic limit of the metal was less than the torque adjusted in the hand piece [7].

Table 1: Properties of NiTi and stainless steel rotary files.

Properties	Ni-Ti alloy	Stainless steel
Ultimate tensile strength	~1240 MPa	~760 MPa
Density	6.45 gm/cm ³	8.03 gm/cm ³
Recoverable elongation	0.08	0.008
Effective modulus	~48 GPa	~193 GPa
Coefficient of thermal expansion	6.6×10 ⁻⁶ -11×10 ⁻⁶ °C ⁻¹	17.3×10 ⁻⁶ °C ⁻¹
Micro-hardness	303-362 VHN	522-542 VHN

Mechanical characteristics and elasticity was enhanced when the nickel titanium alloys was heat treated [8]. Austenite, R phase, and martensite are the phases of nickel titanium alloys. In the martensite phase the nickel titanium files are soft, malleable and easily can be distorted, but shape can be regained when it will be warmed to a degree more than the transformation temperature. The finish degree of temperature for traditional super-elastic is about (16-31°C), when compared with controlled memory wire and M-wire alloys which reveal greater finish temperatures at austenite transformation (55 and 50°C), respectively [6,9]. At human body temperature, the traditional super-elastic NiTi instrument are mainly austenite structure while the heat treated NiTi files are mostly at the martensite phase. Pro Taper Universal (PTU) and Pro Taper Gold (PTG) rotary files have same design; but, PTG files have dissimilar metallurgy supported by heat-treatment techniques to improve elasticity, flexural fracture resistance, and higher durability [10]. Pro Taper Next (PTN) files made by M-wire technology, in which the plain nickel titanium wires are thermomechanically treated. The fracture resistance for PTN files has been improved by the unique unsymmetrical rotary action and decreasing the touching between the file and the root canal walls [4].

Cyclic fatigue of rotary endodontic files tested by the application of bending during rotational movement, many devices and methods were applied for the NiTi rotary endodontic to evaluate the flexural fatigue resistance. The principal measuring methods which used to measure the shape of the canal are the curvature (radius and angle). Some investigators showed that the collected data could be not trustworthy or logical if the guidelines of the machine didn't respect the shape and design of the instrument [5,7]. In order to avoid these mishaps, simulated canals (0.1-0.3 mm more than the measurements of the file need to be tested [11,12]. For pro taper universal and pro taper gold, the design of S1 file to enlarge the coronal area of the canal, S2 file to enlarge the middle area of the canal. In spite of, S1 and S2 shaping files were designed to prepare the upper two thirds of the root, but they make also preparation for the coronal area of the apical part. F1, F2 and F3 finishing files are responsible for more preparation for the middle part and complete preparation for the apical part [13]. So we think that we need to make the file design Plain (free of flutes) in the part which supposed not to be responsible in the canal preparation.

MATERIALS AND METHODS

Study design

The Shaping files (S1 and S2) have small-sized tips that act as guides to passively follow the path of the canal previously secured with hand files. Increasingly larger percentage tapers over the active length of each file

ensures shaping the coronal and middle thirds. The Finishing files (F1) have fixed tapers from D1 to D3, and then decreasing percentage tapers from D4 to D16. This design feature limits the Finishing files to working in their apical extents and reduces the possibility of overpreparing the coronal two-thirds of a canal.

The recommended design modification is to leave the apical 8 mm of file S1 as blank shaft with round cross section (un-milled), and the apical 3 mm of file S2 un-milled, whereas for files F1 only the apical 5 mm would have cutting blades leaving the middle and coronal portions un-milled (bladeless). For the pro taper next files is to leave the apical 8 mm of file X₁ file blank shaft with round cross section (un-milled) while for X₂ files is to leave the coronal 8 mm as blank shaft with round cross section (un-milled) (Figure 1).

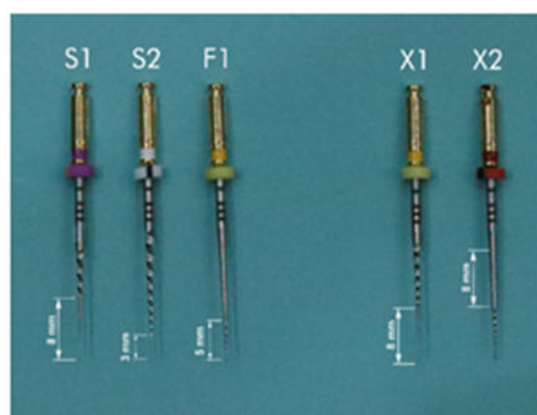


Figure 1: shaping files of the study design.

Preparation of artificial canals

Artificial canals have been machined in plates made from stainless-steel and the dimensions were (100 mm, 50 mm, 10 mm) by utilizing the laser micromachining technology. For machining LASERTEC 40 (Deckel Maho Gildemeister, Ger.) was used, and it comprises of Q-switched Neodymium-doped Yttrium Aluminum Garnet (Nd: Y3 Al5 O12) (Nd: YAG) laser. The artificial canal that is to be machined has been modeled with the use of the CATIA V-5® program and laser path programming has been done with a Standard Triangle Metals language file of proprietary machine program, which operated at a 1064 nm wavelength with a peak power equal to 30. Laser was concentrated on the metal piece by using the galvano scanner after the establishment of parameters for laser processes, and then layer by layer the canal was then machined [14]. In stainless-steel blocks, the artificial canals were machined with similar dimensions to the specifications of the file examined to avoid the file's binding in the testing apparatus 0.1 mm wide and +0.2 mm deep, allowing for some lateral movement within the canal. For dimensions determination, a straight line was drawn along the long axis of canal's coronal

section at a 45-degree angle. A 2nd line is drawn along apical section of canal's long axis. Each of these lines has a point where the canal deviation starts (point a) or ends (pointb) the canal curvature.

A circle with tangents at locations a and b represents the canal's curving segment. The number of the degrees on arc of circle between a and b points (Figures 2-4) (with a radius of 5 mm and a curvature centre 5 mm from the instrument tip) is the angle of curvature (Figure 2) [5,7].

As indicated in Table 2, the PTU and PTG equipment dimensions have been reported based on the instructions of the manufacturer.

The manufacturer's exact dimensions for the PTN, as well as maximal PTN instruments' diameters, as it has been measured with Digimizer[®] program have been listed in Table 3.

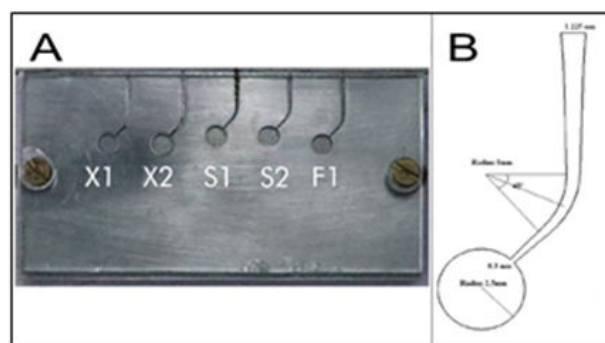


Figure 2: Custom-made stainless-steel blocks with dimensions corresponding to the dimensions of Pro Taper Next (X1, X2), Pro Taper Gold (PTG), and pro taper universal (PTU) (S1, S2, F1): +0.1 mm in width and +0.2 mm in depth, with an angle of curvature of 45°, a radius of curvature of 5 mm, and a centre of curvature 5 mm from the tip of the instrument (A); (B) Two-dimensional draft of artificial canal.

Table 2: Dimensions of PTU and PTG from the manufacturer.

Active part length (mm)	Diameter (mm)		
	S1	S2	F1
0	0.17	0.2	0.2
1	0.19	0.24	0.27
2	0.22	0.34	0.34
3	0.26	0.335	0.41
4	0.305	0.39	0.465
5	0.355	0.45	0.52
6	0.415	0.51	0.575
7	0.485	0.57	0.63
8	0.565	0.63	0.685
9	0.655	0.69	0.74
10	0.755	0.76	0.795
11	0.855	0.85	0.85
12	0.96	0.955	0.905
13	1.075	1.07	0.96
14	1.185	1.185	1.015
15			1.07
16			1.125

Table 3: Dimensions of the PTN from the manufacturer.

Active part length (mm)	Diameter (mm)			
	X1		X2	
	Actual	Maximum	Actual	Maximum
16	1.16	1.26	1.2	1.3
13	0.98	1.06	1.11	1.15
9	0.7	0.76	0.84	1.06
6	0.49	0.534	0.63	0.7
3	0.31	0.35	0.43	0.45
1	0.21	0.23	0.31	0.34
0	0.17	0.17	0.25	0.25

Cyclic fatigue testing

Group number 1: Ten instruments of each pro taper universal S1, S2, F1 (Dentsply Mail filler), ten instruments of each S1, S2, F1 for simulated pro taper universal and ten files for each S1, S2, F1 for pro taper universal study design totally 90 pieces.

Group number 2: Ten instruments of each pro taper gold files S1, S2, F1 (Dentsply Mail filler), ten instruments of each S1, S2, F1 for simulated pro taper universal and ten files for each S1, S2, F1 for pro taper universal study design totally 90 pieces.

Group number 3: Ten instruments of each pro taper next X1, X2 (Dentsply Mail filler), ten files of X1 and X2 for simulated pro taper next files, and ten files of X1 and X2 for simulated pro taper next study design files totally 60 pieces. A main frame with stainless-steel blocks was affixed to which a moveable support for the hand piece was linked. As illustrated in Figure 2, the dental hand-piece has been installed on movable device which allowed for easy deployment of every tool inside artificial canal. The artificial canals were coated with glass for the purpose of preventing instruments from slipping out and for allowing the observation of instruments. In an artificial canal, the instruments were revolved until they fractured. The time till the instrument fractured was recorded using a timer. The speed of rotation as recommended by the manufacturer (300 rpm) until fracture.

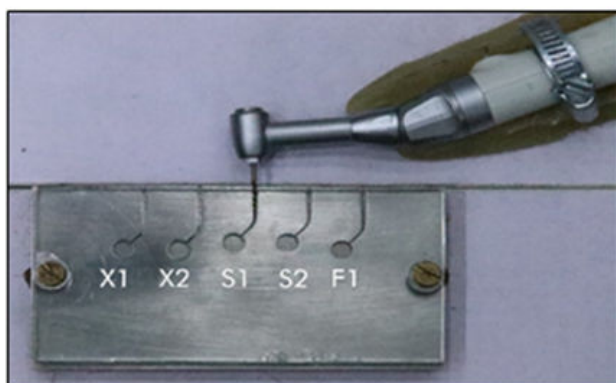


Figure 3: CF testing device illustrating positioning of dental hand piece, NiTi rotary instrument, and stainless steel block.

The instrument was observed and viewed through the glass throughout each test until it fractured, and time to the fracture has been recorded in seconds. Rotary files prior to and post fracture are shown in Figure 3. When the instrument fractured, the electric motor button was pressed again to stop the action. The shattered file was replaced with a new one once the slide was opened (Figure 4).



Figure 4: Fractured files.

Statistical analysis of the empirical data is essential for the proper interpretation and prediction of results. In this work, one-way ANOVA and Tukey’s tests were performed to analyse and compare the means. Statistical significance was set at $P < 0.05$ [15,16].

RESULTS

Pro taper universal

Descriptive statistics of cyclic fatigue fracture of pro taper universal files (Dentsply, Simulated and study) are presented in Tables 3-8.

The results showed that for S1 and S2 files the Dentsply mean values were higher than Simulated and study groups, while for F1 files the simulated mean values were higher than Dentsply and study. Statistical comparisons among the groups were performed using

one way ANOVA test among all S1 and F1 files groups revealed a statistically high significant difference (P<0.001) and non-significant difference among S2 files groups.

Table 4: Descriptive statistics of Cyclic fatigue fracture values of pro taper universal groups in Seconds.

Pro taper universal	Descriptive statistics	Comparison	Mean	SD	95% confidence interval		Minimum	Maximum	F-test	P-Value
					LB	UB				
					S1	Dentsply				
	Simulated	118	8.419	111.977	124.023	104	129			
	Study	132.5	7.472	127.154	137.845	124	146			
S2	Dentsply	103.1	6.951	98.127	108.072	91	115	2.142	0.137	
	Simulated	98.9	8.748	92.641	105.158	88	114			
	Study	100.9	10.246	93.57	108.229	85	115			
F1	Dentsply	79.1	6.063	74.762	83.437	69	89	80.285	0	
	Simulated	110.7	7.318	105.464	115.935	99	121			
	Study	73.9	7.607	68.457	79.342	64	89			

Further comparisons were performed using Tukey's HSD test and the results for S₁ files groups revealed high significant difference (P<0.001) between Dentsply and Simulated groups, and between Dentsply and study group, while it was significant difference (P<0.05) in values between study and Simulated groups.

For F1 files groups revealed a high significant difference (P<0.001) in values between Dentsply and Simulated group, and between study and Simulated group, while no significant difference (P>0.05) in values between Dentsply and study group, which shown in Tables 2 and 3.

Table 5: Tukey HSD among groups of each type of pro taper universal files.

Pro taper universal	Mean difference	P-Value	95% confidence interval		
			LB	UB	
S1	Dentsply - Simulated	44.4	0.000 (H.S)	34.792	54.007
	Dentsply - Study	29.9	0.000 (H.S)	20.292	39.507
	Simulated - Study	-14.5	0.002 (S)	-24.1	-4.892
F1	Dentsply - Simulated	-31.6	0.000 (H.S)	-39.393	-23.8
	Dentsply - Study	5.2	0.241 (N.S)	-2.593	12.993
	Simulated - Study	36.8	0.000 (H.S)	29.006	44.593

Pro taper gold

Descriptive statistics of cyclic fatigue fracture of pro taper gold files (Dentsply, Simulated and study) are presented in Table 6. The results showed that for S1 files the study mean values were higher than Simulated and dentsply groups, while for S2 and F1 files groups the Dentsply mean values were higher than simulated and

study, Statistical comparisons among the groups were performed using one way ANOVA test and the results showed statistically high significant difference (P<0.001) in all files groups.

Table 6: Descriptive statistics of cyclic fatigue fracture values of pro taper gold groups in seconds.

Protaper gold	Descriptive statistics	Comparison	Mean	S.D.	95% Confidence Interval		Minimum	Maximum	F-test	P-Value
					LB	UB				
					S1	Dentsply				
	Simulated	219.8	14.512	209.418	230.181	202	241			
	Study	263.4	16.8	251.381	275.418	244	286			
S2	Dentsply	202.7	14.575	192.273	213.126	178	229	38.555	0	
	Simulated	157.9	10.332	150.508	165.291	140	171			
	Study	163.7	11.944	155.155	172.244	142	178			
F1	Dentsply	198.5	16.574	186.643	210.356	181	225	15.617	0	

Simulated	163.9	12.022	155.299	172.5	148	182
Study	178	12.736	168.888	187.111	157	194

Further comparisons were performed using Tukey's HSD test and the results for S1 files groups revealed a non-significant difference ($P>0.05$) in values between Dentsply and Simulated group, while was high significant difference ($P<0.001$) in values between Dentsply and study group, and between study and Simulated groups. For S2 files groups results revealed a high significant difference ($P<0.001$) in values between Dentsply and Simulated groups and between Dentsply and study groups, and a non-significant difference ($P>0.05$) in

values between study and Simulated groups. For F1 files revealed a high significant difference ($P<0.001$) in values between Dentsply and Simulated groups, significant difference ($P<0.05$) in values between Dentsply and study groups, and a non-significant difference ($P>0.05$) in values between study and Simulated group which shown in Table 7.

Table 7: Tukey HSD among groups of pro taper gold files.

Pro taper gold	Mean difference	P-Value	95% confidence interval		
			LB	UB	
S2	Dentsply - Simulated	-11.4	0.277 (N.S)	-29.452	6.652
	Dentsply - Study	-55	0.000 (H.S)	-73.052	-36.947
	Simulated - Study	-43.6	0.000 (H.S)	-61.652	-25.547
F1	Dentsply - Simulated	44.8	0.000 (H.S)	31.041	58.558
	Dentsply - Study	39	0.000 (H.S)	25.241	52.758
	Simulated - Study	-5.80	0.555 (N.S)	-19.558	7.958

Pro taper next

Descriptive statistics of cyclic fatigue fracture of pro taper next files (Dentsply, Simulated and study) are presented in Table 8. The results showed that for both X1 and X2 files the Dentsply mean values were higher than

Simulated and study groups, Statistical comparisons among the groups were performed using one way ANOVA test among all X1 and X2 files groups revealed a statistically high significant difference ($P<0.001$).

Table 8: Descriptive statistics of Cyclic fatigue fracture values of pro taper next groups in Seconds.

Protaper next	Descriptive statistics	Comparison	Mean	S.D.	95% Confidence interval		Min.	Max.	F-test	P-Value
					LB	UB				
					X1	Dentsply				
X2	Simulated	128.2	11.321	120.101	136.299	114	145	17.853	0	
	Study	158.2	11.679	149.845	166.554	141	175			
	Dentsply	132.6	33.583	108.576	156.623	102	183			
X1	Simulated	92.7	11.719	84.316	101.083	79	111	76.365	0	
	Study	78.4	7.7917	72.826	83.974	69	90			
	Dentsply	193.1	12.242	184.342	201.857	179	212			

Further comparisons were performed using Tukey's HSD test and the results for X1 files groups revealed high significant difference ($P<0.001$) between all groups. For X2 files groups results revealed a significant difference ($P<0.05$) in values between Dentsply and Simulated

group, and high significant difference between Dentsply and study groups, while no significant difference ($P>0.05$) in values between simulated and study group, which shown in Table 9.

Table 9: Tukey HSD among groups of each type of pro taper next files.

Protaper Next		Mean difference	P-Value	95% Confidence interval		
				LB	UB	
X1	Dentsply	Simulated	64.9	0.000 (H.S)	51.867	77.933
		Study	34.9	0.000 (H.S)	21.867	47.933
	Simulated	Study	-30	0.000 (HS)	-43.033-	-16.967
X2	Dentsply	Simulated	39.9	0.001 (S)	16.589	63.21
		Study	54.2	0.000 (H.S)	30.889	77.51
	Simulated	Study	14.3	0.297 (N.S)	-9.01	37.61

DISCUSSION

The instruments used in the presented work have been chosen due to the fact that they all followed the same instrumentation scheme. In comparison to PTN and PTU series, the PTG series exhibited better CF behaviour in this work. The axes of rotation, cross sections, tapering schemes, and metallurgic processing alterations of PTG, PTU, and PTN instruments, on the other hand, differ.

PTG instruments were considered as the most CF-resistant, succeeded by PTN as well as PTU. Also, the thermomechanical treatment related to PTN and PTG instruments might be linked to their high CF resistance. PTG has more flexibility compared to PTU in this work, which is due to the thermal treatment regarding NiTi alloy, which promotes flexibility and prevents crack propagation through preventing the crystallography slipping. In the case when all other criteria (design, cross section, and so on) are the same, a file that is more flexible might experience a lower amount of the stress for certain strain, which allow long fatigue lifetime. In addition, the number of the loading cycles necessary for developing a fatigue crack and propagating the crack to a critical size is the component's fatigue life [8]. Instrument morphology is thought to be a considerable predictor of CF behaviour, which could indicate why PTG instruments have a higher CF resistance than PTN instruments. A few researchers have found that instrument design isn't a significant factor of CF resistance [17]. While others indicated that the cross-sectional design of different files is a major determinant of CF resistance [9,11,12,18,19]. Instruments with a triangle cross-section showed stronger fatigue resistance in comparison to those with square cross-section, according to [20].

CF resistance of various NiTi rotary systems has been compared in many researches. Utilizing a 3-point bending device at 40 curvature and radius of 6 mm, Hieawy, et al. investigated the CF resistance regarding PTG as well as PTU instruments of sizes S1 to F3. Their findings have shown that PTG file had a considerably high CF resistance in comparison to PTU files (P<0.001). Despite the fact that the PTU and PTG systems have the same operation and architecture, the instruments' varied manufacturing procedures have a significant impact on their fatigue resistance behaviours and stress-strain distribution patterns. The transformation behaviour related to NiTi alloys is strongly influenced by their thermomechanical treatment. Based on the thermomechanical treatments, the martensitic transformations in the near-equiatomic NiTi alloys could be a single stage transformation (Austenite (A) Marten

site (M) or a 2-phase transformation (A-R-M) [21]. In Ni-rich NiTi alloys, a one-stage transformation A-to-M takes place, then a two-stage transform A-R-M takes place following more heat treatments that results in finely dispersed Ti₃Ni₄ precipitates in the austenitic matrix [22].

When indicating that an R-phase is one other possible phase of the marten site and the relative preferences regarding R-phase over the marten site in the presence of the fine particles, the transformation from one-stage into two-stage may be understood. This is due to the fact that Ti₃Ni₄ particles are resisting the development of marten site, related to a substantial deformation of the lattice, yet they resist the creation of R-phase, related too much smaller deformation of the lattice, far less. Although the existence of Ti₃Ni₄ particles encourages the R-phase formation, the alloy must be cooled further to create marten site. As a result, martensitic transformation takes place in two stages: A-R-M [21]. In the case when stress is applied over a critical threshold, which occurs in the case where the ambient temperature is over the material's Af temperature, pseudo-elasticity or super-elasticity is connected with the phase transformation occurrence regarding NiTi alloy. To employ pseudo-elasticity, the working temperature for standard super-elastic NiTi files should be higher than Af. Actually, the Af temperatures of super elastic NiTi files, such as Pro Taper and Pro File, are below body temperature [8]. The variations in the resistance to fatigue between PTU and PTG files are explained by the occurrence of such variations of the marten site that might be linked to high transformation temperature degrees that have been reported in PTG files. The number of the cycles to the failure in the martensitic NiTi wires could be 100 times high compared to that in stable as well as super elastic austenitic NiTi, according to [22]. PTG has been more adaptable than PTU in this investigation. In the case when all other criteria (design, cross section, and so on) are the same, a higher flexibility file might experience lower level of stress for a certain strain, which allow long fatigue lifetime.

The number of the loading cycles that are necessary for developing a fatigue crack and propagating the crack to critical size is the component's fatigue life. In marten site, the mechanism of crack propagation consists of a huge number of extremely branched cracks which propagate slowly. Just some cracks nucleate in super elastic NiTi, and they propagate quickly [23]. Furthermore, in both the PTU and PTG systems, the S2 and S1 files showed high resistance to fatigue failure in comparison with F-1-F-3 files (P<0.001). The results from PTG and PTU series

in [6]. Indicated that that S1 PTG had the maximum CF resistance of all files (P less than 0.001); therefore, the higher the level of the strain (typically represented by the instrument radius ratio at the point of the breakage to curvature radius), the shorter becomes the fatigue life. In addition, the S-1 PTU files had statistically significantly more sufficient cyclic fatigue resistance in comparison to F2, F1, and F3 files, according to previous tests. This has been also validated in the current work, which found that as instrument diameter increased, both PTU and PTG showed decreased fatigue resistance [24]. In our study, for pro taper universal results, Dentsply showed the highest mean values than simulated and study files for S1 files, while for F1 files showed least mean difference but no significant difference for S2 files and, for pro taper gold results Dentsply showed no significant difference in mean values than simulated files for F1 files, while highest mean values for S2 files and for F1 files, also highest mean values for pro taper next results in both tested files X1 and X2 which might be due to various factors like the manufacturing processes and alloy's chemical composition [25,26]. Different inclusion particles, such as oxide particles, are incorporated on the metal surface throughout the process of manufacturing. These particles serve as a nucleating site for micro crack propagation [27]. According to cracks propagate perpendicular to the instrument's long direction, and micro voids are occasionally generated on the surface due to the presence of nitrogen, oxygen, carbon and hydrogen [28]. More cracks might form along such faults, and in the case when exposed to unloading and loading of instrument, those areas undergo a phase transition from austenitic to martensitic, affecting the instrument's mechanical properties [29]. While S1 study files showed higher mean values than simulated files for both pro taper universal and pro taper gold groups which attributed to the curvature area in the simulated canal is (5 mm) from the apex and plane part of study file is (8 mm) from the apex of the file making it more resistant to fracture because its plane (unthreaded) in which the area between the spiral and adjacent spiral act as a weak area which is more susceptible to fracture, this agree with One of the researches had shown that dentinal debris has been mostly wedged in the narrow radial, land-type areas and less on convex flute surfaces of the utilized Pro Taper files [27]. Dentinal debris has been found predominantly in metal rollover and on the concave flute surfaces in an examination of used Pro File instruments.

Those dentinal chips can lead to a build-up of tensions, which can lead to NiTi rotary instruments failing clinically. Also, the clinical fracture related to NiTi rotary instruments is thought to be induced primarily by a single overload throughout instrumentation, instead of severe alloy fatigue. Local dentinal chip embedment in machining grooves can produce such overloading [30]. S2 study files indicated no significant difference from simulated files for both pro taper universal and pro taper gold groups which attributed to the curvature area in the simulated canal is (5 mm) from the apex and plane part of study file is (3 mm) from the apex so the area at curvature of simulated and study files are both with

spirals at this part of the file. F1 study files showed less mean values than simulated files for pro taper universal group which attributed to the area of curvature in simulated canal is (5 mm) from the apex and plane part of study file is (5 mm) from the apex so the curvature of simulated canal at the level of the connection of the plane and spiral part which act as a weak area. This is consistent with Pruett who found that instruments subjected to cyclic fatigue fractured at the centre of curvature or just below it, as previously described [5]. F1 study files showed no significant difference in mean values than simulated files for pro taper gold group in spite of curvature in the simulated canal is (5 mm) from the apex and plane part of study file is (5 mm) from the apex so the curvature of simulated canal at the level of the connection of the plane and spiral part which act as a weak area but the heat treatment of pro taper gold files make the results differ from pro taper universal this is agree with Xu X who said that many factors might impact the stress distribution in NiTi instruments like the alloy, design, and the heat treatment applied throughout manufacturing [31,32].

For pro taper next results, X1 study files showed higher mean values than simulated files which attributed to the curvature area in simulated canal is (5 mm) from the apex and plane part of study file is (8 mm) from the apex of the file making it more resistant to fracture because its without spirals in which the area between the spiral and adjacent spiral act as a weak area which is more susceptible to fracture, Alapati SB showed that depth of flutes or increase the number of spirals of the flute per unit length decrease torsional resistance [27]. X2 study files showed lower mean values than simulated files which may be attributed to that it is with (8 mm) with flutes from the apex and the remaining (8 mm) of the shaft is plane without flutes which affect the flexibility of the file and loose its eccentric rotation of the pro taper next which shows a rectangular cross-section design with regard to superior strength as well as excellent asymmetric rotary motion which enhances the effectiveness of canal shaping as indicated *via* the manufacturer. Furthermore, they are created with the use of M-Wire NiTi for enhancing the flexibility and cyclic fatigue resistance of files (Dentsply Maillefer, Ballaigues, Switzerland).

CONCLUSION

The PTG instruments were most resistant to CF, followed by PTN and PTU. The higher CF resistance of the PTG and PTN instruments can be attributed to the thermomechanical treatment of these instruments. For PTU and PTG files groups, for S1 and S2 files making the non-active part plane will increase CF resistance while for F1 files will decrease CF resistance. For PTN files groups, for X1 files making the non-active part plane will increase CF resistance while for X2 files will decrease CF resistance.

REFERENCES

1. Walia H, Brantley W, endodontics HGJ, et al. undefined An initial investigation of the bending and torsional properties of Nitinol root canal files. *J Endodontics* 1998; 14: 346-351.
2. Hulsmann M, Peters OA, Dummer PMH, et al. Mechanical preparation of root canals: shaping goals, techniques and means. *Endod Top* 2005; 10:30-76.
3. Anous W, Al-Ashry S, Ali M, et al. Effect of different kinematic cutting motion in multiple versus single-file concept on dentinal crack formation: An *in vitro* study. *J Int Oral Heal* 2020; 12:30-40.
4. Elnaghy AM, Elsaka SE. Assessment of the mechanical properties of ProTaper next nickel-titanium rotary files. *J Endod* 2014; 40:1830-1834.
5. Pruett O, John P, David J, et al. Scientific Articles Cyclic Fatigue Testing of Nickel-Titanium Endodontic Instruments 1997; 23:77-85.
6. Hieawy A, Haapasalo M, Zhou H, et al. Phase transformation behavior and resistance to bending and cyclic fatigue of ProTaper Gold and ProTaper Universal instruments. *J Endodontics* 2021; 41:1134-1138.
7. Plotino G, Grande NM, Cordaro M, et al. A Review of Cyclic Fatigue Testing of Nickel-Titanium Rotary Instruments. *J Endodontics* 2009; 35: 1469-1476.
8. Shen Y, Zhou H-M, Zheng Y-F, et al. Current Challenges and Concepts of the Thermomechanical Treatment of Nickel-Titanium Instruments. *J Endod* 2013; 39:163-172.
9. Haikel Y, Serfaty R, Bateman G, et al. Dynamic and cyclic fatigue of engine-driven rotary nickel-titanium endodontic instruments. *J Endod* 1999; 25:434-440.
10. Ruddle C, Machtou P, today JW-D, et al. undefined Endodontic Canal Preparation: New Innovations in Glide Path Management and Shaping Canals. Accessed J 2021.
11. Plotino G, Grande NM, Sorci E, et al. A comparison of cyclic fatigue between used and new Mtwo Ni-Ti rotary instruments. *Wiley Online Libr* 2006; 39:716-723.
12. Gambarini G, Grande N, Plotino G, et al. Fatigue resistance of engine-driven rotary nickel-titanium instruments produced by new manufacturing methods. 2008 ;34:1003-1005.
13. Capar I, Kaval M, Ertas H, et al. Comparison of the cyclic fatigue resistance of 5 different rotary pathfinding instruments made of conventional nickel-titanium wire, m-wire, and controlled memory wire. 2015 ;41:535-538.
14. Mohammed MK, Al-Ahmari A, Umer U, et al. Multiobjective optimization of Nd:YAG direct laser writing of microchannels for microfluidic applications. *Int J Adv Manuf Technol* 2015; 81:1363-1377.
15. Correia J de O, Pedrosa B, Engineering PR, et al. Fatigue strength evaluation of resin-injected bolted connections using statistical analysis. 2017 ;3:795-805.
16. Correia J, Blasón S, ADJ-EF, et al. Fatigue life prediction based on an equivalent initial flaw size approach and a new normalized fatigue crack growth model. 2016 ;69:15-28.
17. heung GSP, Darvell BW. Low-cycle fatigue of NiTi rotary instruments of various cross-sectional shapes. *Int Endod J* 2007; 40:626-632.
18. Ray JJ, Kirkpatrick TC, Rutledge RE, et al. Cyclic fatigue of endo sequence and k3 rotary files in a dynamic model. 2007; 33:1469-1472
19. Tripi T, Bonaccorso A, Surgery GC-O, et al. Cyclic fatigue of different nickel-titanium endodontic rotary instruments. 2006 ;102:106-114.
20. Cheung GSP, Zhang EW, Zheng YF, et al. A numerical method for predicting the bending fatigue life of NiTi and stainless steel root canal instruments. *Int Endod J* 2011; 44:357-361.
21. Sarkar S, Ren X, Otsuka K, et al. Evidence for strain glass in the ferroelastic-martensitic system Ti50-xNi50+x. *Phys Rev Lett* 2005; 95.
22. Figueiredo A, Modenesi P, Fatigue VB-IJ, et al. Low-cycle fatigue life of super elastic niti wires. 2009; 31:751-758.
23. McKelvey AL, Ritchie RO. Fatigue-crack growth behavior in the superelastic and shape-memory alloy nitinol. *Metall Mater Trans A*. 2001; 32:731-743.
24. Pérez-Higueras JJ, Arias A, de la Macorra JC, Peters OA. Differences in cyclic fatigue resistance between ProTaper Next and ProTaper Universal instruments at different levels. *J Endod* 2014; 40:1477-1481.
25. Kuhn G, Jordan L. Fatigue and mechanical properties of nickel-titanium endodontic instruments. *J Endod* 2002; 28:716-720.
26. Marending M, Lutz F, Barbakow F, et al. Scanning electron microscope appearances of Light speed instruments used clinically: A pilot study. *Int Endod J* 1998; 31:57-62.
27. Alapati S, Brantley W, Svec T, et al. Proposed role of embedded dentin chips for the clinical failure of nickel-titanium rotary instruments. Elsevier 2021.
28. Alapati S, Brantley W, Svec T, et al. Sem observations of nickel-titanium rotary endodontic instruments that fractured during clinical use. Elsevier 2021.
29. Miyai K, Ebihara A, Hayashi Y, et al. Influence of phase transformation on the torsional and bending properties of nickel-titanium rotary endodontic instruments. *Int Endod J* 2006; 39:119-126.

30. Madarati AA, Watts DC, Qualtrough AJE, et al. Factors contributing to the separation of endodontic files. *Br Dent J* 2008; 204:241-245.
31. Xu X, Eng M, Zheng Y, et al. Comparative study of torsional and bending properties for six models of nickel-titanium root canal instruments with different cross-sections. *J Endod* 2006; 32:372-375.
32. Johnson Matthey (Inspiring science, Enhancing life). Nitinol and stainless steel: property comparison. 2017.